UNIVERSITAT POLITÈCNICA DE VALÈNCIA

DEPARTAMENTO DE MATEMÁTICA APLICADA

KTH ROYAL INSTITUTE OF TECHNOLOGY

DEPARTMENT OF MECHANICS

High-order spectral simulations of the flow in a simplified urban environment: A study of flow statistics

PABLO TORRES GREUS

MASTER THESIS FOR MSC. IN MATHEMATICAL RESEARCH

DIRECTOR : DR. SERGIO HOYAS CALVO

DR. RICARDO VINUESA MOTILVA

Contents

Introduction

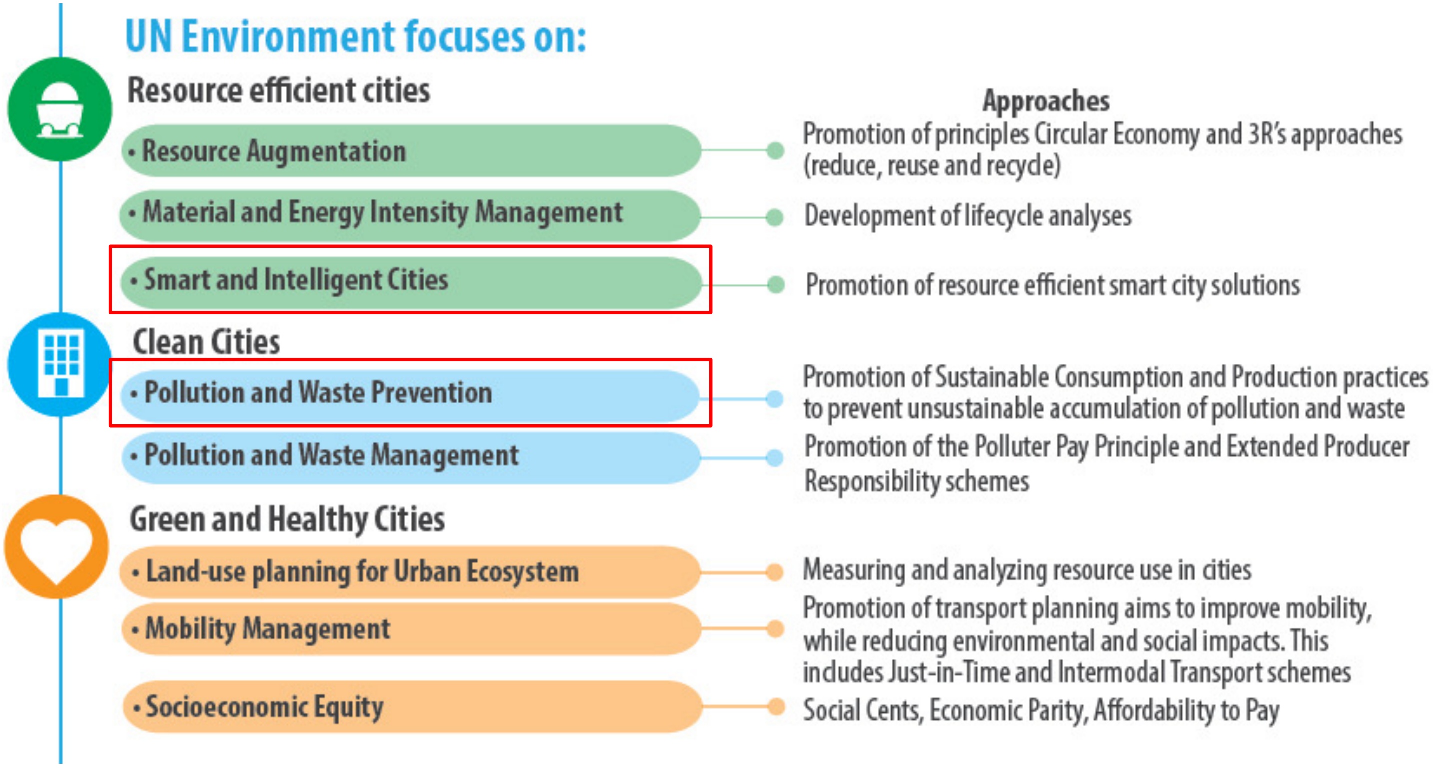

Fig. 1 . Sustainable cities. United Nations Environment Program. Retrieved from UN Regional Initiatives.

Fig. 2 . SDG 11. United Sustainable development program. Retrieved from UN Sustainable Development Communications materials.

Objectives

1. Identify and study the relevant processes and factors in urban turbulent flows
2. Develop and integrate the meshing and solution processes
3. Design the geometry and mesh
4. Set the simulation strategy and parameters
5. Obtain the time-averaged quantities
6. Analyse and appraise resolution and boundary-layer quantities
7. Analyse and discuss the obtained flow behaviour for the three flow regimes

Historical perspective

Experimental methods

- Full-scale experiments:
  - Carried out in open environments.
  - Typically involves large and expensive equipment.
  - Typically used in local studies.
  - *e.g.:* Hirose *et al.*[1] presented a project was to study wind-induced natural ventilation in cities and how those are a ected by the surroundings urban flows

- Reduced-scale experiments:
  - Carried out in open and confined environments.
  - They are simpler than full-scale experiments but they tend to miss out important processes.
  - They are limited by the fact that the behaviour of the flow in controlled environments tends to differ from the behaviour of the flow in open environments.
  - *e.g.:* Weerasuriyaa *et al.*[4] presented a study on the e ect of twisted winds at a pedestrian level using a scaled model of the Tsuen Wan street in Hong Kong inside a boundary layer windtunnel.

Historical perspective

Numerical simulations

- Modelling numerical techniques: RANS and others
  - Only the mean flow is solved, everything else is modelled.
  - The computational cost is reduced but the accuracy of the solutions is very limited.
  - *e.g.:* Lien *et al.*[2] presented a work focusing on the predictive capabilities of modelling techniques within the frame of urban environments.

- Direct numerical simulations (DNS):
  - No modelling involved. All the scales are solved.
  - It is the most accurate method but it is very expensive computationally.
  - *e.g.:* Vinuesa *et al.*[3] simulated the flow over a wall-mounted square cylinder using a DNS.

- Large-eddy simulation (LES):
  - Only the smallest scales of the turbulence are modelled. The rest of the scales (which carry the majority of the energy) are solved.
  - With a strict resolution criteria it can deliver results very close to the results obtained with a DNS with a much lower computational cost.
  - It is the prefered choice in urban flow simulations since simulations tend to be large and the convergence very slow.

Theoretical Background

Governing equations

Navier-Stokes equations:

$$\frac{D\boldsymbol{U}}{Dt} = -\frac{1}{\rho}\nabla p + \nu\nabla^2\boldsymbol{U} \quad (1)$$

Reynolds equations:

$$\left\langle\frac{DU_j}{Dt}\right\rangle = \frac{\partial}{\partial x_i}\left[\mu\left(\frac{\partial\langle U_i\rangle}{\partial x_j} + \frac{\partial\langle U_j\rangle}{\partial x_i}\right) - \langle p\rangle\delta_{ij} - \rho\langle u_i u_j\rangle\right] \quad (2)$$

Budget equation:

$$B_{ij} \equiv \frac{D\langle u_i u_j\rangle}{Dt} = P_{ij} + \varepsilon_{ij} + T_{ij} + \Pi_{ij}^s + \Pi_{ij}^d + V_{ij} \quad (3)$$

Reynolds decompositon

Fields are decomposed in the mean and fluctuation term:

$$\boldsymbol{U}(\boldsymbol{x},t) = \langle\boldsymbol{U}(\boldsymbol{x},t)\rangle + \boldsymbol{u}(\boldsymbol{x},t) \quad (4)$$

Budget terms

$$\begin{aligned} P_{ij} &= -\langle u_i u_k\rangle U_{jk} - \langle u_j u_k\rangle U_{ik} \\ \varepsilon_{ij} &= -2\mu\langle u_{ik} u_{jk}\rangle \\ T_{ij} &= \langle u_i u_j u_k\rangle_k \\ \Pi_{ij}^s &= \langle p(u_{ij} + u_{ji})\rangle \\ \Pi_{ij}^d &= -[\langle p u_i\rangle\delta_{jk} + \langle p u_j\rangle\delta_{ik}] \\ V_{ij} &= \mu\langle u_i u_j\rangle_{kk} \end{aligned} \quad (5)$$

Theoretical Background

Boundary layer parameters

The boundary layer is the layer of fluid in the immediate vicinity of a bounding surface.

Momentum thickness and Reynolds number

$$\theta = \int_0^{+\infty} \frac{U(y)}{U_\infty}\left(1 - \frac{U(y)}{U_\infty}\right) dy \quad (6)$$

$$Re_\theta = \frac{U_\infty \theta}{\nu} \quad (7)$$

Shear stress and friction coefficient

$$\tau_w = \mu \left(\frac{dU}{dy}\right)_w \quad (8)$$

$$C_f = \frac{\tau_w}{\frac{1}{2}\rho U_\infty^2} \quad (9)$$

Normalisation

We use "+" units to normalise quantities:

Friction velocity

$$u_\tau = \sqrt{\tau_w/\rho} \quad (10)$$

Spatial grid-spacing

$$\Delta x^+ = \frac{u_\tau \Delta x}{\nu} \qquad \Delta y^+ = \frac{u_\tau \Delta y}{\nu} \quad (11)$$

$$\Delta z^+ = \frac{u_\tau \Delta z}{\nu}$$

Velocity and fluctuations:

$$U^+ = U/u_\tau \qquad u^+ = u/u_\tau^2 \quad (12)$$

Tools and setups

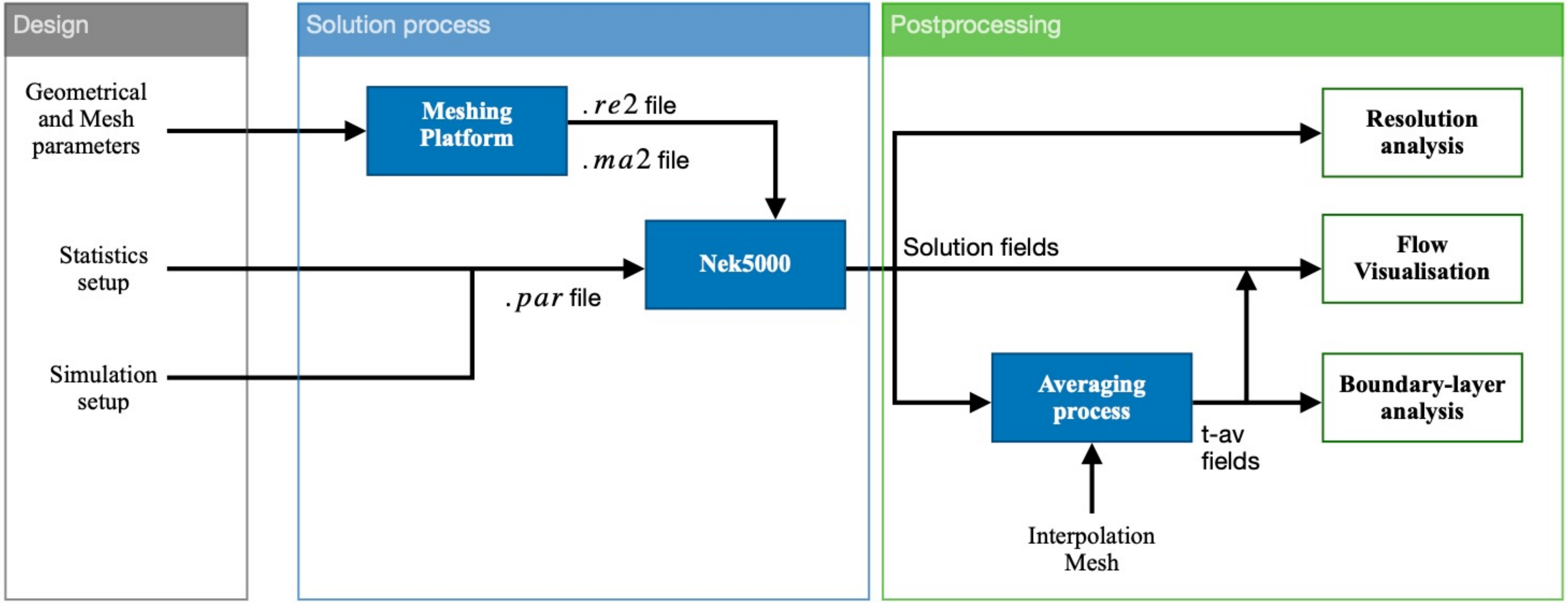

Fig. 3. Design, solution and postprocessing scheme

Final simulation setup

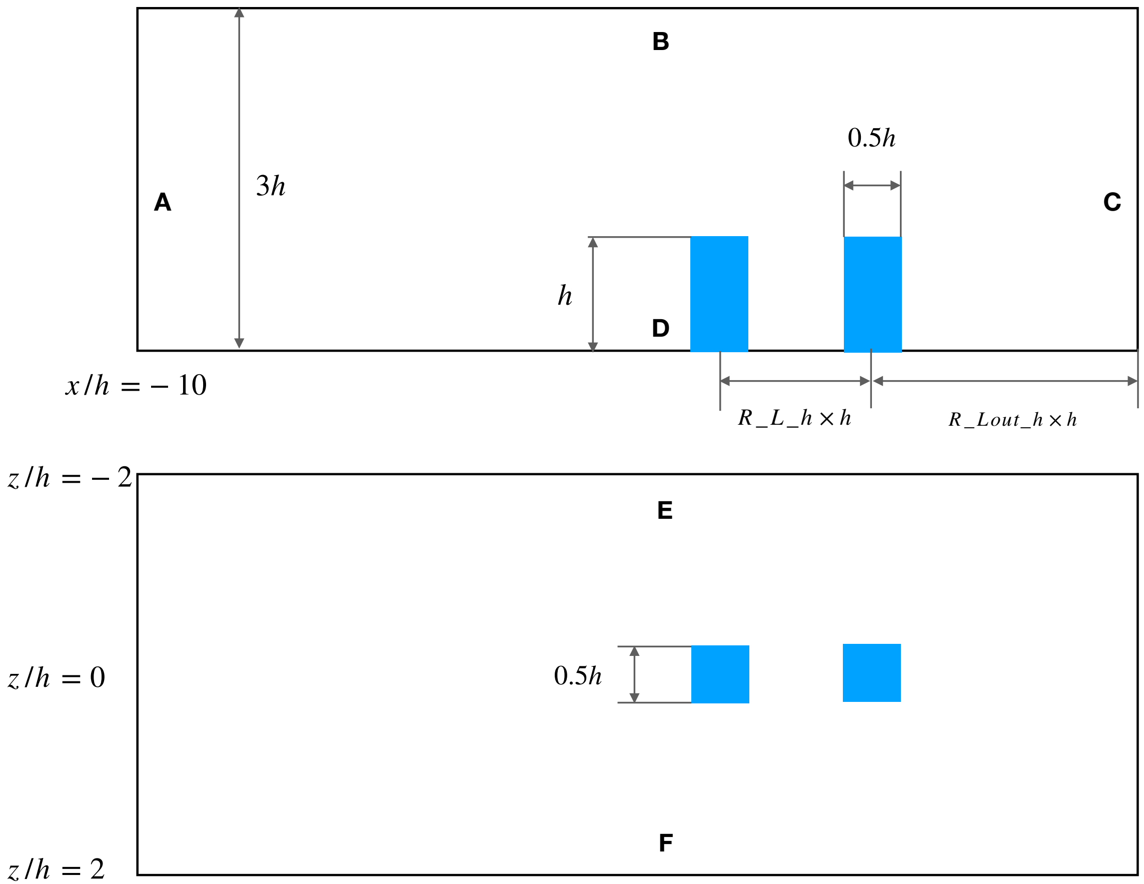

Fig. 4. Diagram showing the final geometry design.

Key information

- Three cases are considered, *i.e.* Skimming Flow (SF), Wake Interference (WI) and Isolated Roughness (IR).
- The sole difference between the cases is the distance between the obstacles.
- 205 605 elements
- 105 M points in total
- Resolution in the near-obstacle region:
  - $\Delta x^+_{n.o.} \approx 10$
  - $\Delta y^+_{n.o.} \approx 0.18$
  - $\Delta z^+_{n.o.,mean} \approx 5$

Boundary-layer & Resolution analysis

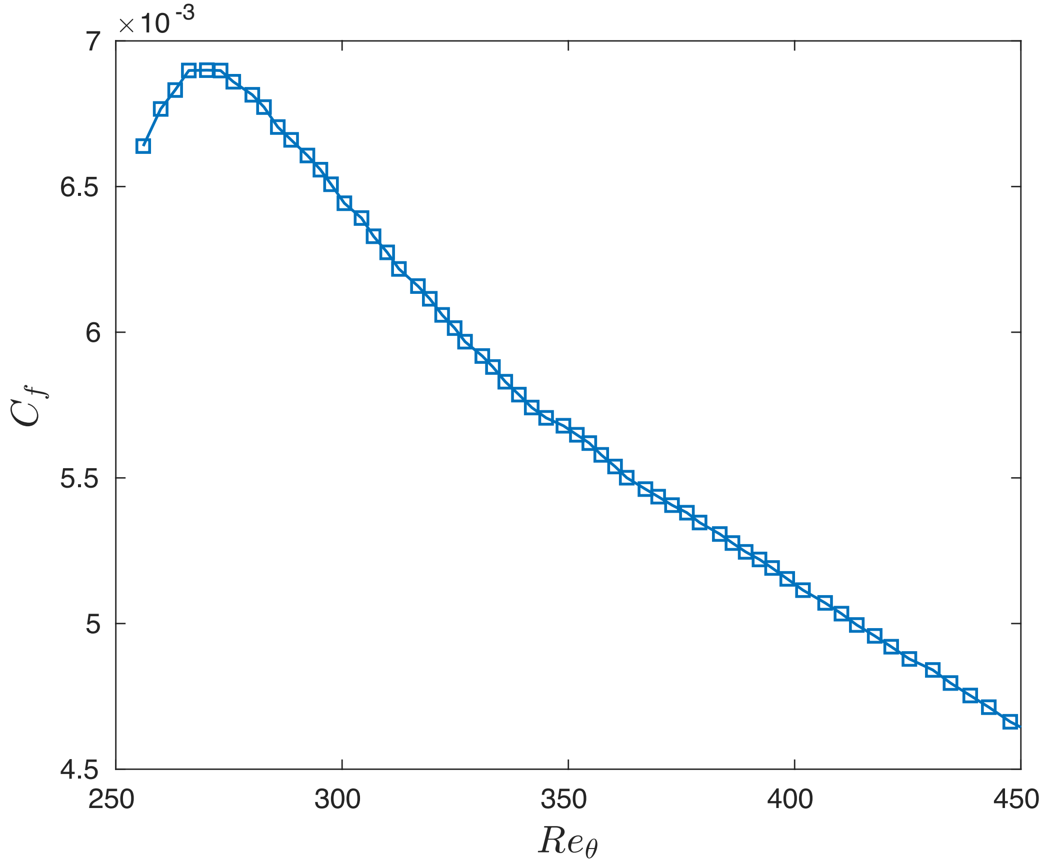

Fig. 5. z-averaged friction coefficient evolution with the Reynolds number evaluated using the momentum thickness for the skimming flow case.

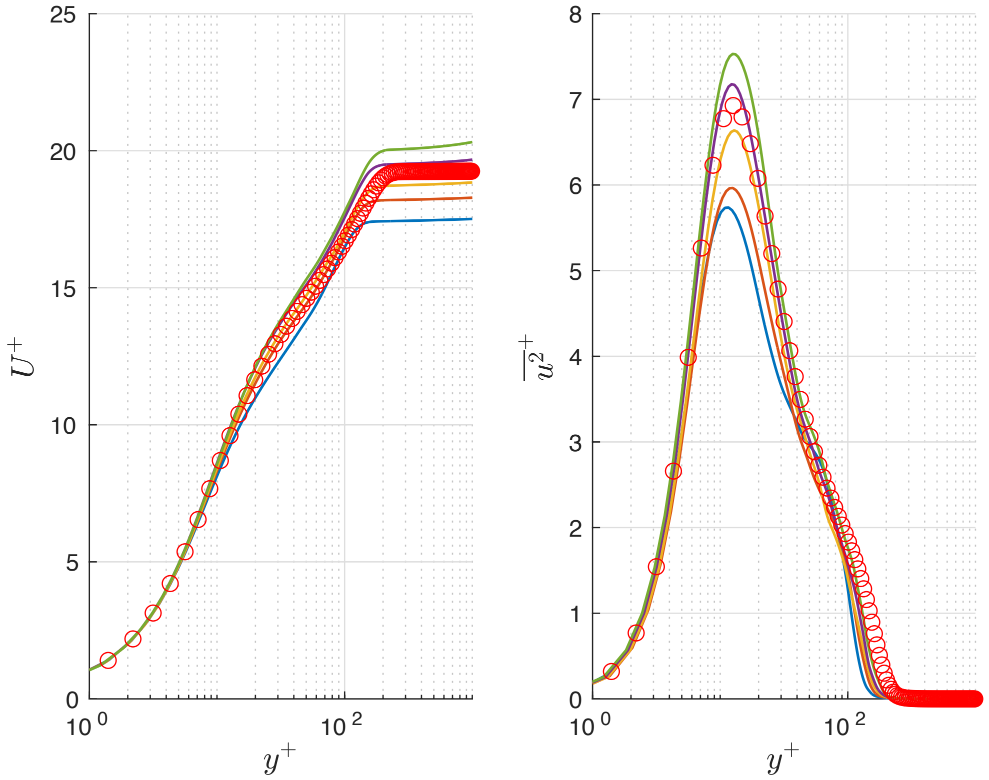

Fig. 6. Normalised z-averaged streamwise velocity (left) and Reynolds-stress tensor component (right) for the skimming flow case.

Results

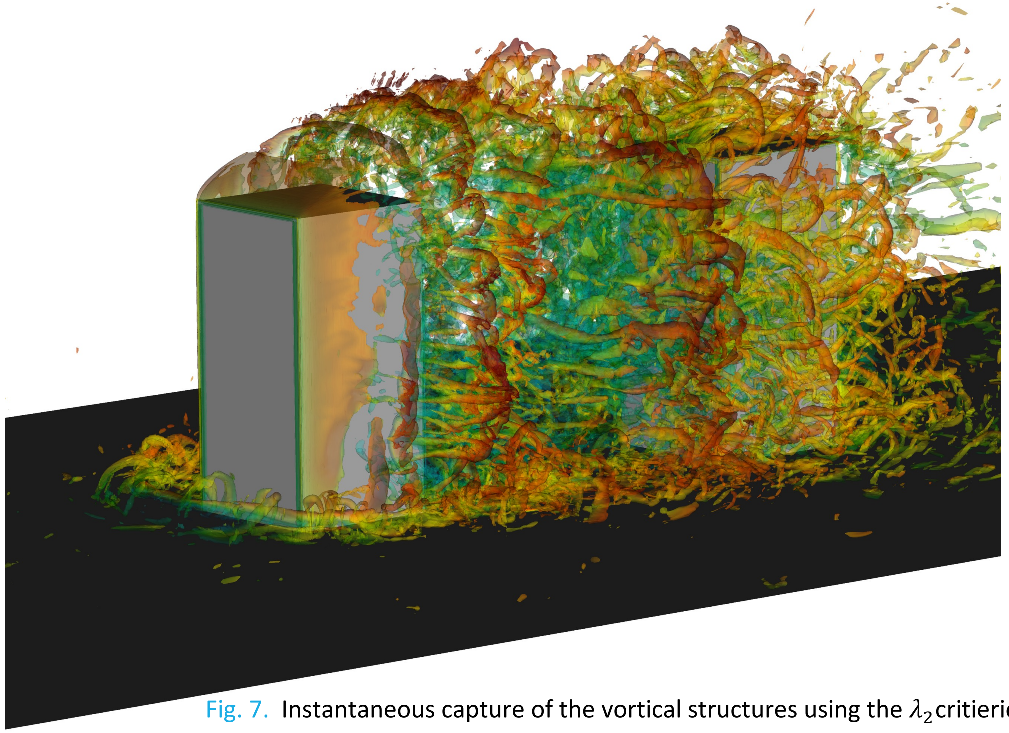

Fig. 7. Instantaneous capture of the vortical structures using the λ_2 critierion.

Vortex indentificaton

Vortical structures are defined using the λ_2 criterion which is defined as the second eigenvalue of the matrix $\boldsymbol{S}^{\mathbf{2}} + \boldsymbol{\Omega}^{\mathbf{2}}$.

$$\boldsymbol{S} = \frac{\nabla \boldsymbol{U}(\boldsymbol{x}, t) + \nabla \boldsymbol{U}(\boldsymbol{x}, t)^T}{2} \quad ; \boldsymbol{\Omega} = \frac{\nabla \boldsymbol{U}(\boldsymbol{x}, t) - \nabla \boldsymbol{U}(\boldsymbol{x}, t)^T}{2}$$

A point of a given velocity field is considered to be part of a vortex core the second eigenvalue λ_2 is negative, *i.e.* $\lambda_2 < 0$.

Results

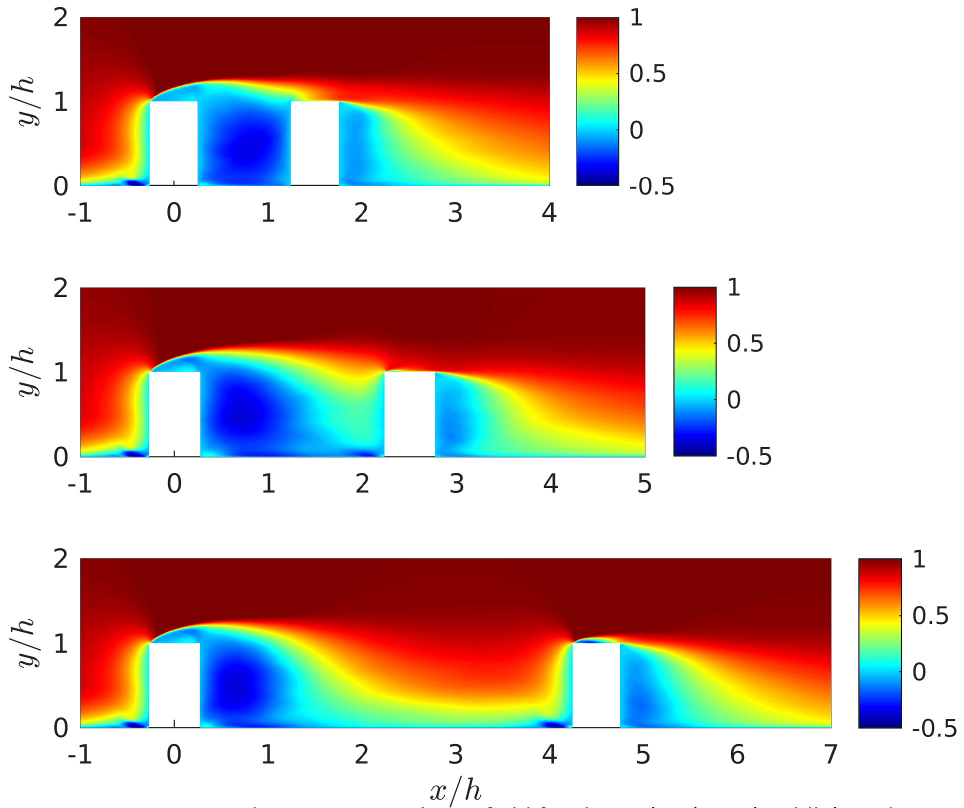

Fig. 8. Time-averaged streamwise velocity field for the SF (top), WI (middle), and IR (bottom) regimes at plane z/h = 0.

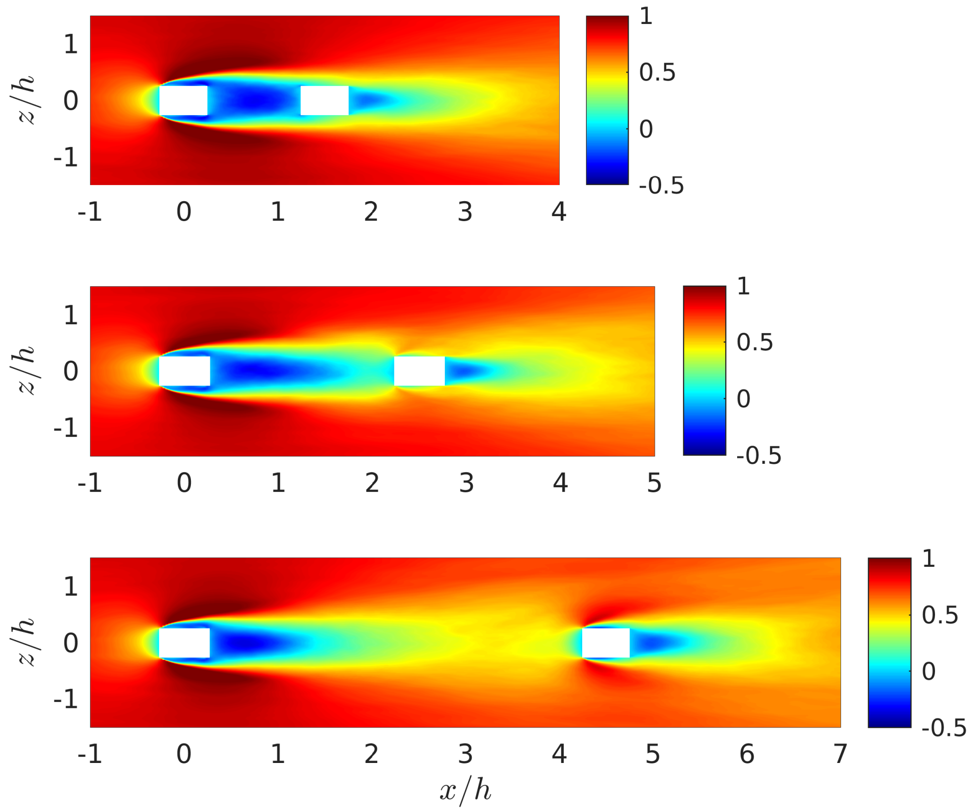

Fig. 9. Time-averaged streamwise velocity field field for the SF (top), WI (middle), and IR (bottom) regimes at plane y/h = 0.25.

Results

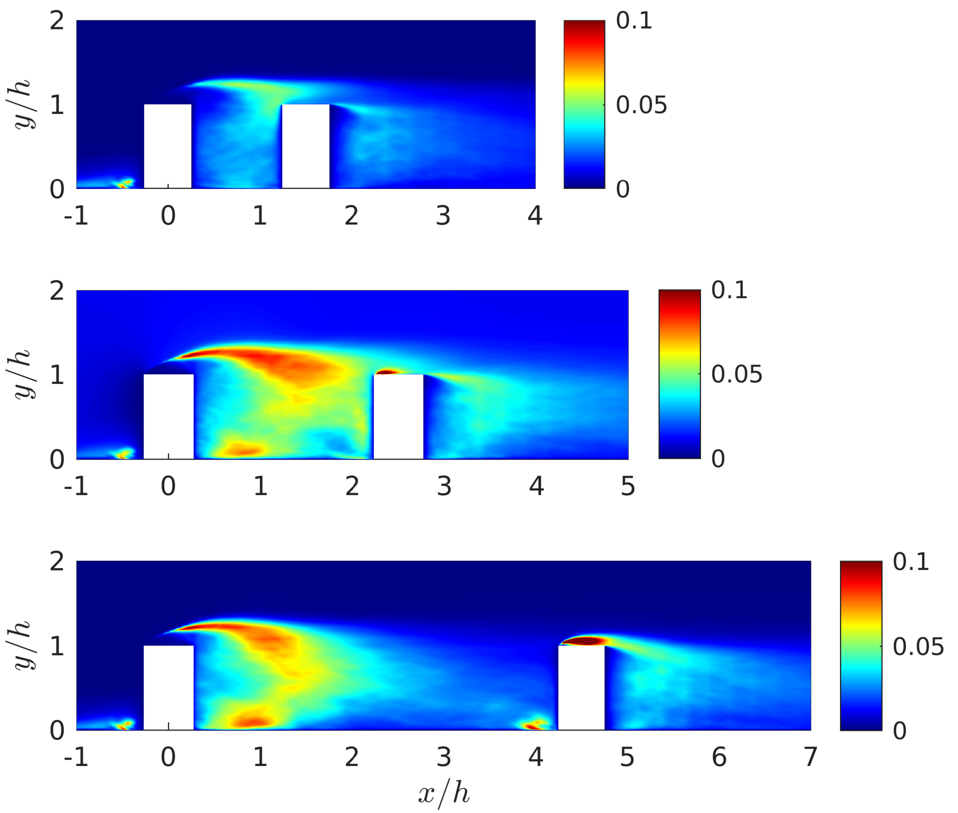

Fig. 10 . Time-averaged Reynolds-stress u^2 component for the SF (top), WI (middle), and IR (bottom) regimes at plane z/h = 0.

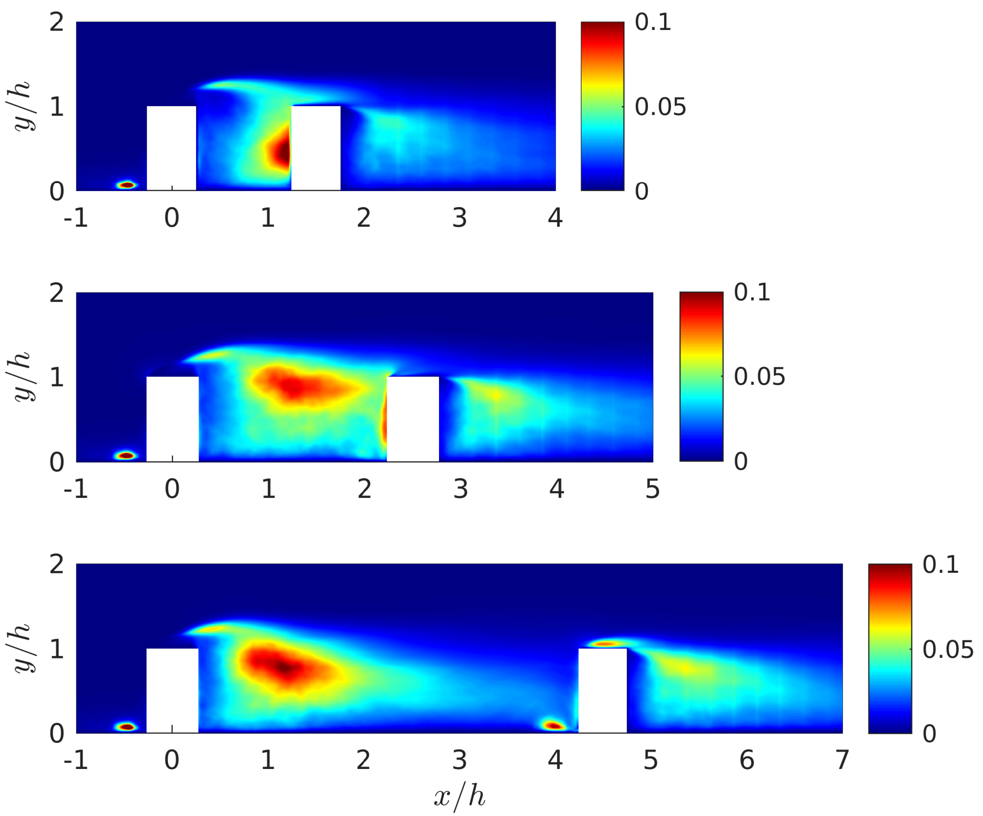

Fig. 11. Time-averaged Reynolds-stress v^2 component for the SF (top), WI (middle), and IR (bottom) regimes at plane z/h = 0.

Results

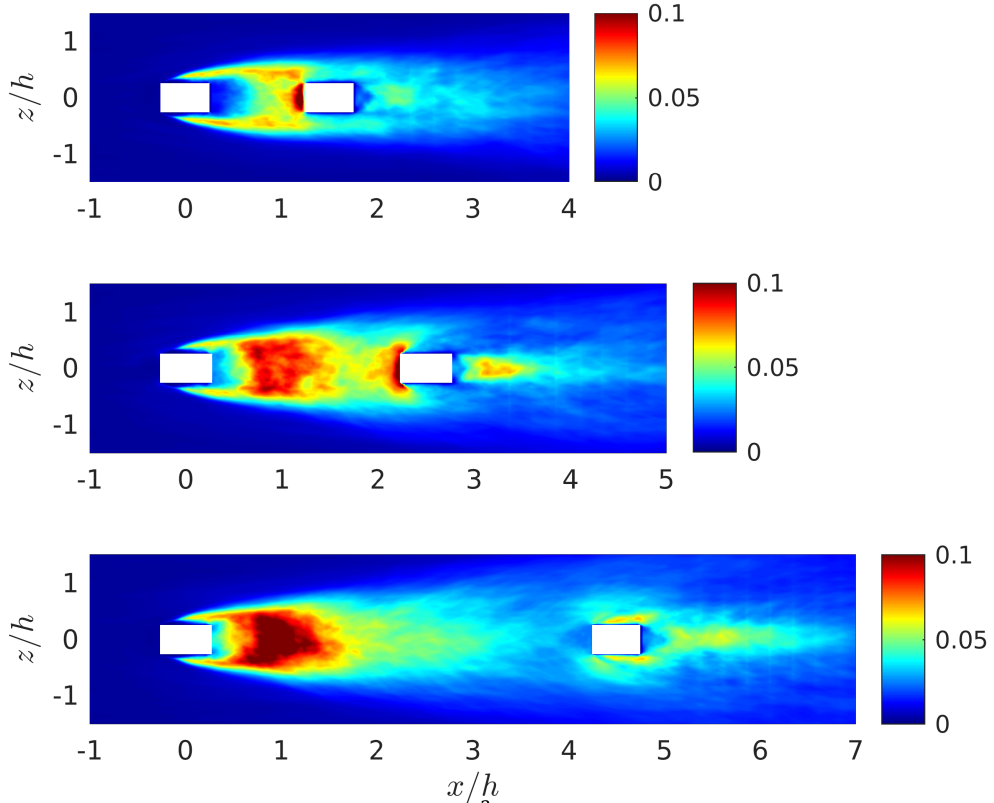

Fig. 12. Time-averaged Reynolds-stress w^2 component for the SF (top), WI (middle)and IR (bottom) regimes at plane y/h = 0.25.

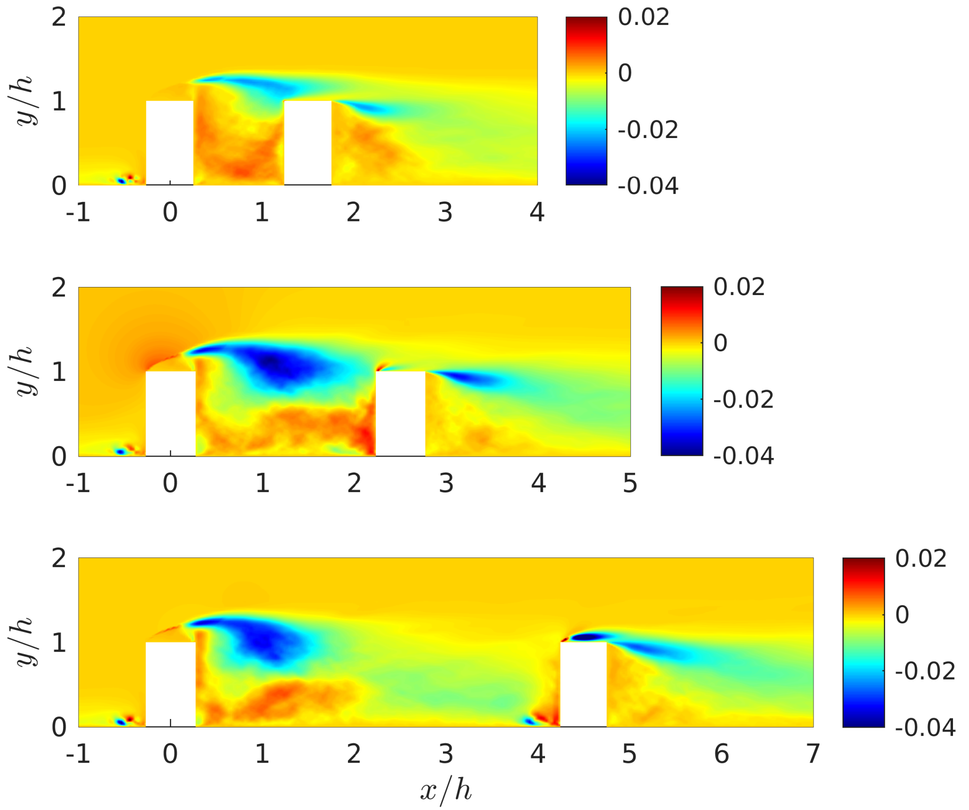

Fig. 13. Time-averaged Reynolds-stress uv component for the SF (top), WI (middle)and IR (bottom) regimes at plane z/h = 0.

Results

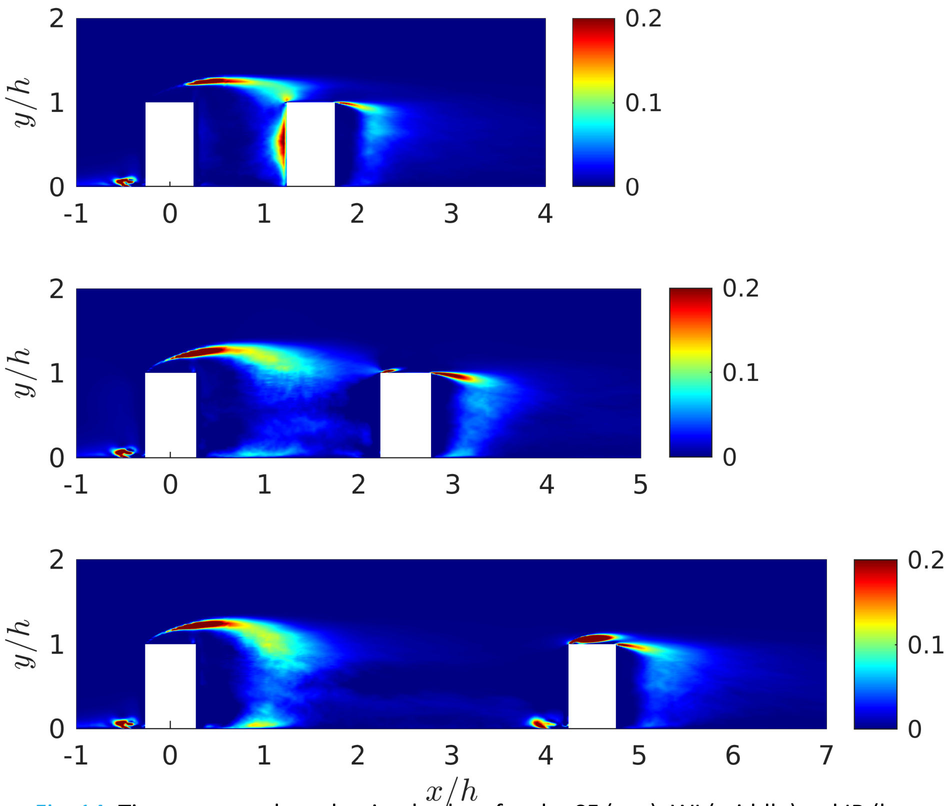

Fig. 14. Time-averaged production budget for the SF (top), WI (middle)and IR (bottom) regimes at plane z/h = 0.

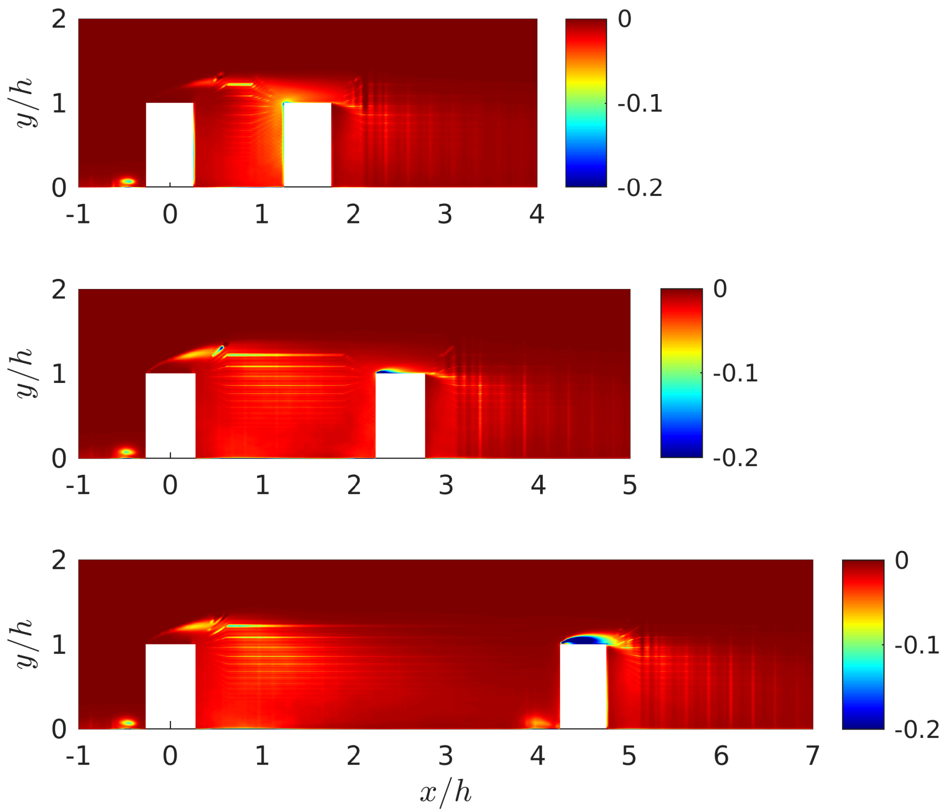

Fig. 15. Time-averaged dissipation budget for the SF (top), WI (middle)and IR (bottom) regimes at plane z/h = 0.

Results

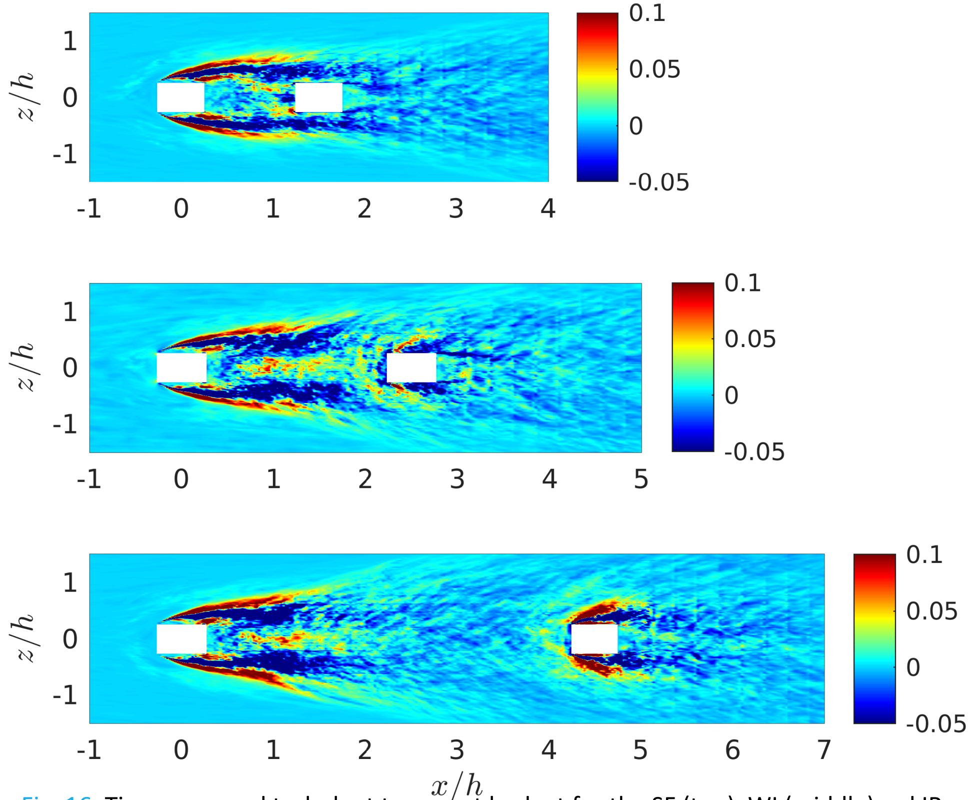

Fig. 16. Time-averaged turbulent transport budget for the SF (top), WI (middle)and IR (bottom) regimes at plane y/h = 0.25.

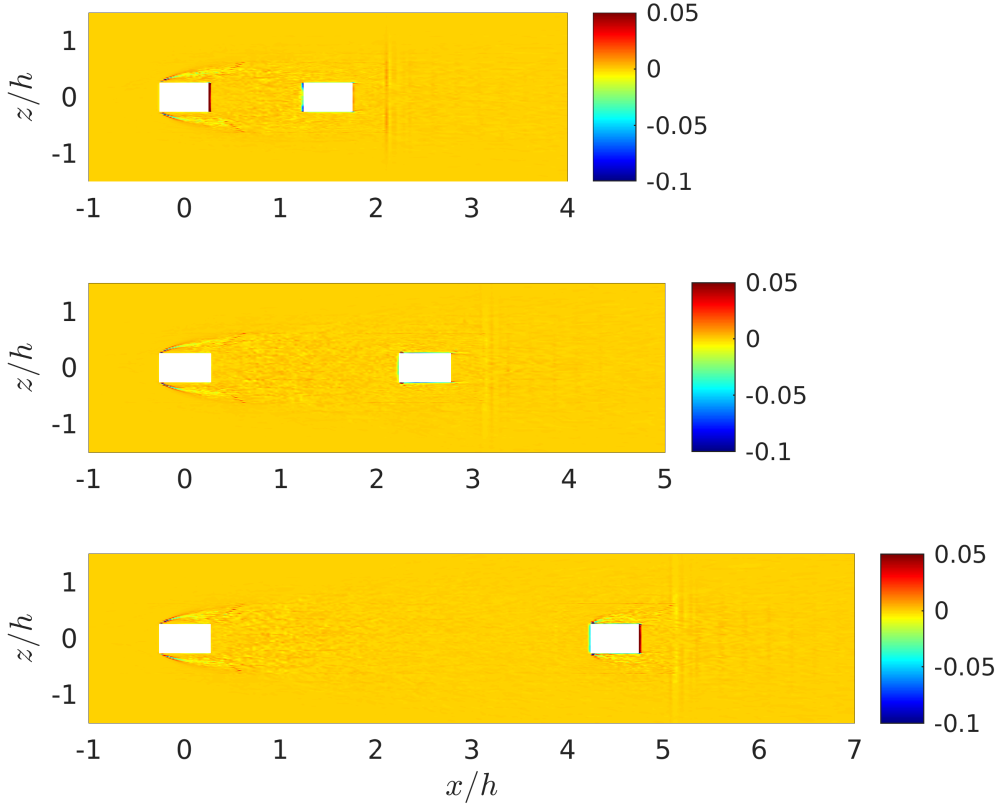

Fig. 17. Time-averaged viscous diffusion budget for the SF (top), WI (middle)and IR (bottom) regimes at plane y/h = 0.25.

Conclusions

1. A well-resolved LES was obtained

2. The mesh was able to properly represent flow and turbulent boundary-layer quantities.

3. Flow behaviour matched theoretical expectations.

4. Simulation results confirm that the distance between the obstacles is the main driver of the flow regimes and that the change in regime has a strong impact on both the velocity and energy of the fluid.

References

[1] Hirose, C., Ikegaya, N., Hagishima, A., and Tanimoto, J. Outdoor measurement of wall pressure on cubical scale model a ected by atmospheric turbulent flow. *Building and Environment 160* (2019).

[2] Lien, F.-S., Yee, E., Ji, H., and Hsieh, K.-J. Partially resolved numerical simulation and RANS modeling of flow and passive scalar transport in an urban environment. *Journal of Wind Engineering and Industrial Aerodynamics* 96 (2008).

[3] Vinuesa, R., Schlatter, P., Malm, J., Mavriplisb, C., and Henningsona,D. S. Direct numerical simulation of the flow around a wall-mounted square cylinder under various inflow conditions. *Journal of Turbulence 16(6)* (2015).

[4] Weerasuriyaa, A., Tsea, K., Zhanga, X., and Lib, S. A wind tunnel study of effects of twisted wind flows on the pedestrian-level wind   eld in an urban environment. *Building and Environment 128* (2018).

Thank you very much for your attention